Development and Validation of Hypersonic Engine Inlet Design Code

Phyo Wai Thaw[#1], Zin Win Thu[#2]

[#]*Department of Propulsion and Flight Vehicles, Myanmar Aerospace Engineering University, Meiktila, Mandalay Region, Myanmar*

Abstract **- This paper describes the numerical investigation of scramjet inlet and validation through computational fluid dynamics (CFD). The scramjet inlet design (SID) program was also developed and used to design a new scramjet inlet geometry which satisfies shock-on-lip (SOL) condition at Mach 3. This inlet design was further tested by means of CFD and the inviscid data showed that it meets SOL condition and reached the required pressure at the isolator exit to get good burning.**

Keywords **- Scramjet, Oblique Shock, Validation, SID, SOL**

Nomenclature

η_{KE_ad}	= adiabatic kinetic energy efficiency
A	= area
l	= cowl's placement from inlet's tip
θ	= deflection, turning angle
ρ	= density
s	= entropy
x_1	= forebody's horizontal length
x_2	= intake ramp's horizontal length
y_2	= isolator's height
M	= Mach number
π_c	= pressure recovery, total pressure ratio
y_1	= scramjet inlet's height
β	= shock wave angle
R	= specific gas constant
γ	= specific heat ratio
P	= static pressure
P_0	= total pressure
T	= temperature
ϕ	= reflected shock wave angle

I. INTRODUCTION

In the late 1950's and early 1960's, many major scramjet development programs were started due to hypersonic air-breathing engines give a more efficient than rockets [1]. By historical data, the first scramjet demonstration took place in 1960 by Ferri et al [2]. The first successful flight test was the HyShot program by University of Queensland in Australia in July 2002 [3]. X-43A set the Guinness World Record for a jet-powered aircraft with a Mach number of 9.6 in November, 2004 [4].

Compared to rockets, the scramjets have much higher specific impulse and do not require an onboard oxidizer, resulting in lower allowable payload weight [1]. The most suitable air-breathing engine cycle for hypersonic flight is the supersonic combustion ramjet, or scramjet. Although the scramjets have many advantages in hypersonic flight, the scramjets do not work and only rockets will do if the mission includes operation beyond the Earth's atmosphere.

A scramjet is a variant of a ramjet which has no moving parts but shock wave is taken for compression. The ramjet is slowed a supersonic airstream to the subsonic speed before entering the combustor whereas a scramjet decelerates the free stream to supersonic flow throughout the entire engine due to lack of normal shock [5].

Ramjets and scramjets can operate efficiently at supersonic and hypersonic speeds, but there tend to be limitations to the range of Mach numbers. The vehicle cannot be accelerated to take off with both the scramjet and ramjet which must be coupled with some additional form of propulsion such as turbojet or rocket. The inefficiencies of slowing the flow down to subsonic speeds make the ramjet difficult to use for speeds exceeding Mach 5 [6]. As flight speed increases above Mach 5, reducing the air to subsonic conditions produces two problems; (1) significantly increased shock losses in the inlet, particularly at the terminal normal shock, and (2) significantly increased flow temperatures in the combustor [1].

There are possible applications for scramjet engines, including missile propulsion, hypersonic cruiser propulsion, and part of a staged space access propulsion system [7]. The main technical challenge is to operate the scramjet engine at the lowest starting Mach number for a hybrid turbojet-scramjet propelled aircraft which could enter service by 2030 [8].

The scramjet is composed of four major components: a converging inlet where free stream is compressed and decelerated, an isolator which protects the inlet from combustor high pressure effects (adverse back pressure), combustor where gaseous fuel is burned with atmospheric oxygen to produce heat and diverging nozzle where the heated air is accelerated to produce thrust [4].

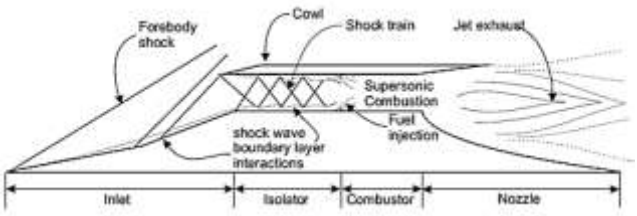

Fig. 1 Schematic diagram of a scramjet engine [14]

II. SCRAMJET INLET

The main purpose of a scramjet inlet is to compress and supply a supersonic flow with suitable pressure, temperature and mass flow rate to combustor for efficient combustion of fuel. It converts kinetic energy to pressure energy. It is a critical component which affects greatly the overall efficiency of the whole scramjet engine because of the thrust loss 1% for each 1% of loss in pressure recovery [9]. The weaker the shock, the smaller the loss in total pressure. The number of intake ramps also influences on total pressure recovery. The total pressure ratio increases if the number of ramps is increased especially more than two or more.

There are three different inlet geometries based on the types of compression: external, mixed and internal as shown in Fig. 2. The shock waves occur outside of isolator utilized a cowl tip angle in the first type of inlet. The second type squeezes the flow by both external and internal shock systems with horizontal cowl tip. The incoming flow is pressurized inside the inlet in the last one. The best choice for minimum external drag on engine cowl is the second type which is parallel to the relative free stream [1].

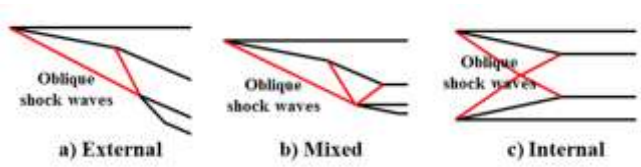

Fig. 2 Different types of compression inlet [1]

A. Inlet Performance Parameters

The performance of air intake is considered into: (1) capability, or how much compression is performed, and (2) efficiency, or what amount of flow losses is occurred during the compression process [1]. Several parameters can be calculated for a scramjet air intake system in order to evaluate its performance. Some of them depend on inlet geometry and the flight operating conditions. Some performance parameters are described by geometric area ratios: (1) air capture ratio (A_1/A_0) is related to the amount of air passing through the engine, (2) aerodynamics contraction ratio (A_1/A_2) is the amount that the flow is squeezed, (3) geometric contraction ratio (A_0/A_2) is related to inlet design [10].

Another parameter related to the inlet adiabatic kinetic energy efficiency (η_{KE_ad}) which doesn't take into account heat loss is calculated. If the kinetic energy efficiency is calculated, the total pressure ratio through the shock wave is needed to be considered. It is the pressure recovery (π_c) which is defined as the stagnation pressure ratio of the compression system. If the difference in total pressure decreases, total pressure recovery increases, and the efficiency is large as shown in the following equation.

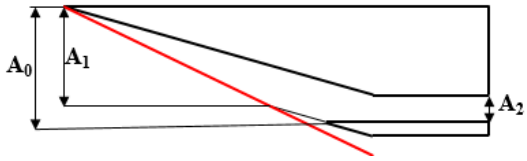

Fig. 3 Scramjet inlet with its relevant areas [12]

According to [11], adiabatic kinetic energy efficiency can be calculated in general as follow:

$$\eta_{KE\_ad} = 1 - \frac{2}{(\gamma-1)M_1^2}\left[\left(\frac{1}{\pi_c}\right)^{\frac{\gamma-1}{\gamma}} - 1\right]$$

B. Compression Requirements

The compression process must be supplied to operate robust combustion process that is required in supersonic combustion. The minimum required combustor inlet pressure is above 50kPa and inlet temperature is above 1000K but the maximum combustor entrance temperature should be in the range of 1440K-1670K to prevent adverse effect of dissociation [1], [11].

The efficient combustion is required shock-on-lip (SOL) condition, which is an important part of inlet design. The SOL condition means that all external oblique shocks hit the cowl tip and reflect exactly to the top corner of the throat as shown in Fig.4 and the shock train is cancelled in the entire region of the isolator [12].

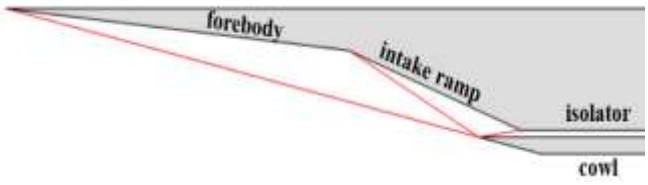

Fig. 4 Air intake system

C. Governing Equations for Design Calculation

The deflection angle and the shock wave angle can be evaluated by the following equations [5], [13].

$$\tan\theta_1 = 2\cot\beta_1\frac{M_1^2\sin^2\beta_1 - 1}{M_1^2(\gamma+\cos 2\beta_1)+1}$$

$$\tan\beta_1 = \frac{M_1^2 - 1 + 2\lambda\cos\left[\left(4\pi\delta + \cos^{-1}\chi\right)/3\right]}{3\left(1+\frac{\gamma-1}{2}M_1^2\right)\tan\theta_1}$$

$$\lambda = \left[\left(M_1^2-1\right)^2 - 3\left(1+\frac{\gamma-1}{2}M_1^2\right)\left(1+\frac{\gamma+1}{2}M_1^2\right)\tan^2\theta_1\right]^{1/2}$$

$$\chi = \frac{\left(M_1^2-1\right)^3 - 9\left(1+\frac{\gamma-1}{2}M_1^2\right)\left(1+\frac{\gamma-1}{2}M_1^2+\frac{\gamma+1}{4}M_1^4\right)\tan^2\theta_1}{\lambda^3}$$

Flow properties behind the oblique shock wave can be calculated by the following equations [5].

$$M_2 = \frac{1}{\sin(\beta_1-\theta_1)}\left[\frac{1+\frac{\gamma-1}{2}M_1^2\sin^2\beta_1}{\gamma M_1^2\sin^2\beta_1-\frac{\gamma-1}{2}}\right]^{1/2}$$

$$\frac{P_2}{P_1} = 1+\frac{2\gamma}{\gamma+1}\left(M_1^2\sin^2\beta_1-1\right)$$

$$\frac{\rho_2}{\rho_1} = \frac{(\gamma+1)M_1^2\sin^2\beta_1}{(\gamma-1)M_1^2\sin^2\beta_1+2}$$

$$\frac{T_2}{T_1} = \frac{P_2}{P_1}\frac{\rho_1}{\rho_2}$$

$$s_2 - s_1 = c_p \ln\frac{T_2}{T_1} - R\ln\frac{P_2}{P_1}$$

$$\pi_c = \frac{P_{02}}{P_{01}} = e^{-(s_2-s_1)/R}$$

III. Numerical Analysis

A. Scramjet Inlet Geometry Selection

Firstly, existing two-dimensional inlet geometry is chosen to do numerical investigation and validation. The chosen design used mixed compression inlet with two ramps in order to minimize base drag. The inlet utilized a double-ramp shape to avoid unnecessary length and weight incurred if an isentropic compression surface is used. Typically, an overall compression efficiency of about 0.9 could be achieved with a 3-shock inlet system [14]. The first Brazilian hypersonic vehicle prototype, the 14-X airplane is chosen as a reference geometry. The reference case considers SOL condition at Mach 7 at 30km altitude [12]. All lengths are in millimetre.

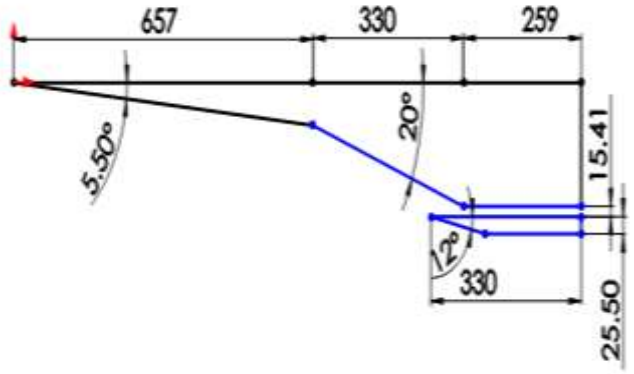

Fig. 5 Reference air intake geometry [12]

B. Computational Domain

For numerical calculations, two dimensional geometry, steady flow, perfect gas, inviscid models for the airflow were considered. Several computational domains with structured grids were constructed and tested in order to get gird independent result. The domain system shown in Fig. 6(e) gave the best result and was used for further investigations.

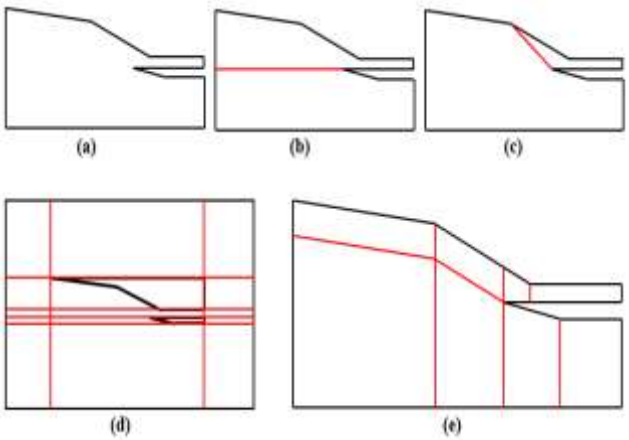

Fig. 6 Various types of computational domain

C. Meshing

For two dimensional computations over the model, a structured grid consisting of quadrilateral cells were used. The grid independence test must be done by transforming the generated physical model into a mesh with different number of node points. It is said to be grid independence when the result doesn't change with increasing grid numbers. The result obtained for this mesh is considered to be the best.

It was found in Fig. 7 that a medium grid of 101369 has a very close fit with the pressure readings from a fine grid of 125720 quadrilateral cells as can be seen in Fig. 8. A coarse grid of 70892 quadrilateral cells also showed close approximation with the other two grid levels as shown in Fig. 8. Therefore, the medium grid level is adopted for all cases considering numerical stability and minimum computational cost. This medium grid resolution used here is sufficient to capture the physically relevant features.

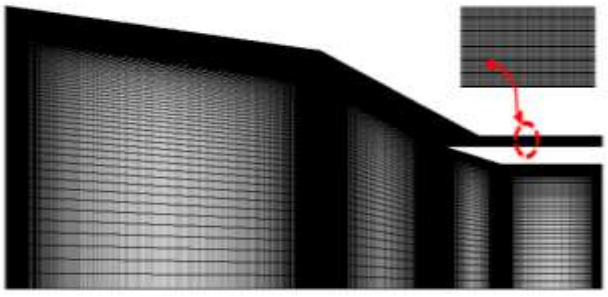

Fig. 7 Medium mesh for the baseline case

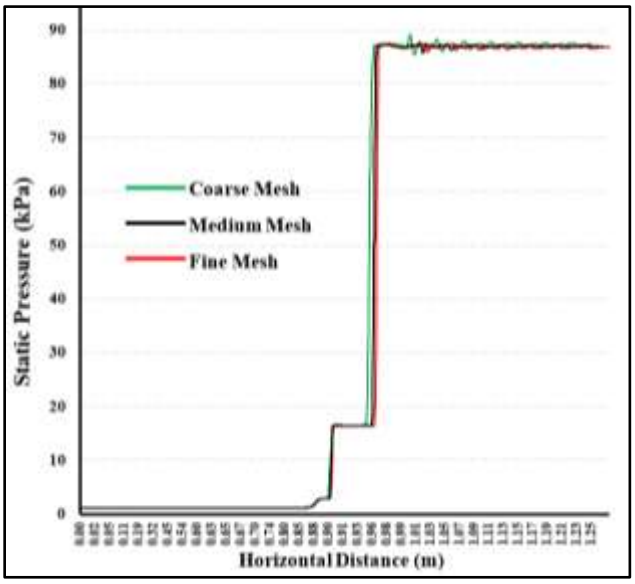

Fig. 8 Static pressure along the center line of scramjet inlet-isolator for case 1 using different grid densities

D. Boundary Conditions

The computational domain is bounded by pressure far-fields, walls and two pressure outlets as shown in Fig.9. The properties for the pressure far-fields are taken from flight operating conditions (TABLEI). Properties at the two pressure outlets were calculated assuming free flow, where the flow would exit the isolator, expanding to free stream conditions.

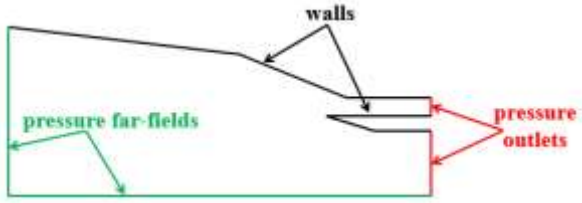

Fig. 9 Boundary conditions

TABLE I
FLIGHT OPERATING CONDITIONS

Case	Flight altitude			Mach number
	H [km]	P [Pa]	T [K]	
1	30	1172	226.65	7
2	30	1172	226.65	8
3	30	1172	226.65	6
4	25	2511	221.65	7
5	35	558.4	237.07	7

E. Convergent Residuals

The numerical solution was converged after approximately 1500 iterations. At this stage, the residuals reach their minimum values after falling for over 6 orders of magnitude.

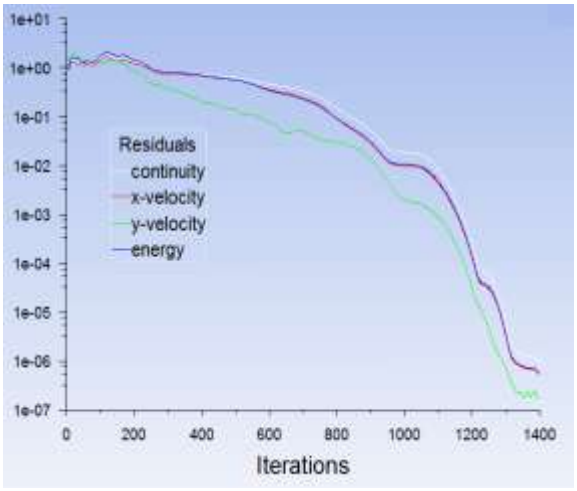

Fig. 10Residuals for scramjet inlet computation

IV. RESULTS AND DISCUSSION

A. Validation

The accuracy of the current numerical investigation was validated with the oblique shock wave relation results for reference case 1. The numerical analysis shows absolutely equal result with inviscid oblique shock analysis result.

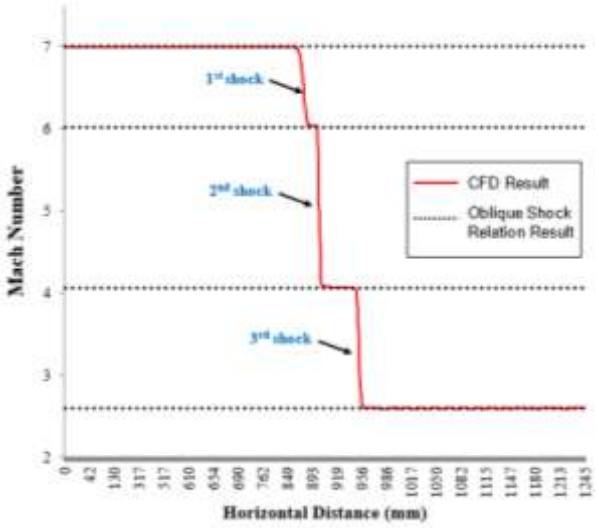

Fig. 11 Validation of Mach number changes across shock waves along horizontal distance

Figs. 11-12 are Mach number changes and pressure changes along horizontal distance from tip of forebody to isolator exit for the case 1 (Mach 7). In Fig. 12, the small amount of pressure fluctuation along isolator was occurred because of the inaccuracy of reference geometry's dimensions that affects SOL condition. The horizontal dashed lines represent the flow properties across oblique shock waves which are calculated by the oblique shockwave relations and the red curve signifies the flow field changes across the shock waves according to the CFD results.

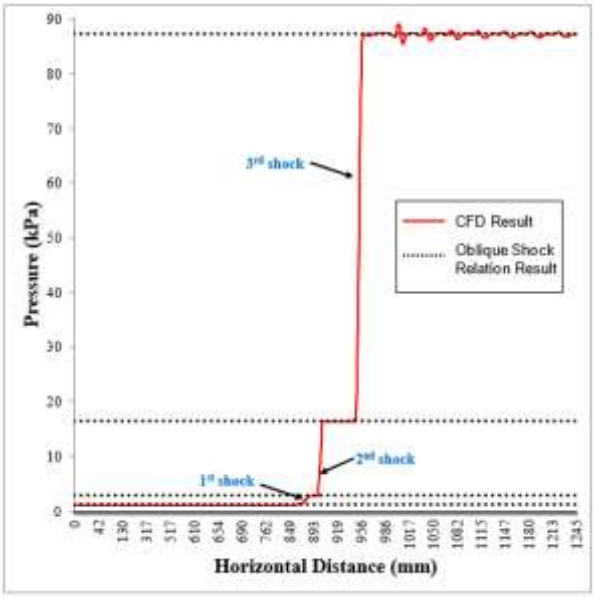

Fig. 12Validation of pressure changes across shock waves along horizontal distance

B. CFD Results

In the numerical analysis, variations of the flight operating conditions such as vehicle speed (represented by Mach number), altitude (pressure, temperature) were considered for the desired constraints. At the flight condition consider the vehicle at Mach 7 in an atmosphere at 30 km altitude, the shock-on-lip condition should be satisfied. The numerical calculation of Mach number contours is shown in Fig. 13 for case 1. Also shown in right upper corner of this figure, is a zoom-in view of the airflow in the isolator. The shock-on-lip really occurs as the oblique shocks from the forebody and inlet ramps hit the cowl tip and reflect exactly to the top corner of the throat. The flow field in the isolator is responded for the combustion process. Fig. 13 shows the reflected shock is cancelled in isolator, which yields uniform airflow property profiles at the combustor entrance. The desired flow properties and greater efficiency are encountered at Mach 7 as shown in TABLEII. The efficient combustion will occur due to the SOL condition.

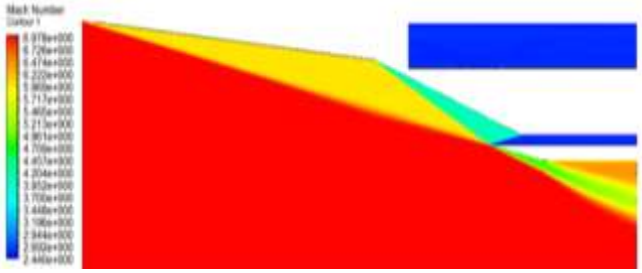

Fig. 13Mach number contour for case 1 (Mach 7)

As can be seen in Figs 14-15, for Mach 8 and Mach 6 cases, the shock-on-lip condition is not satisfied. From θ-β-M relation, the shock wave angle is greater when Mach number is smaller with constant deflection angle whereas the shock wave angle is smaller with increase Mach number from primary Mach number condition.

As shown in Fig. 14, the weaker shocks are generated for Mach 8 than Mach 7 shocks. Since the shock is weak, the first small shock angle which intercepts the second one inside of the isolator so that the SOL condition is not satisfied. Consequently, there are additional shock compression, reflected shocks and flow non-uniformity inside the isolator.

In Fig. 15, for Mach 6, the shock waves are deflected toward outside of the cowl as a result in SOL condition is not satisfied. The stronger shock than Mach 7 which causes some flow spillage and much more pressure losses. In this case, some part of the airflow is not captured by the inlet. Also it causes the reflected shock and flow non-uniformity inside the isolator.

For inviscid flow and calorically perfect gas models, the Mach contours of changing flight altitude (case 4 and case 5) are the same as the one presented in Fig. 13 for the reference case 1.

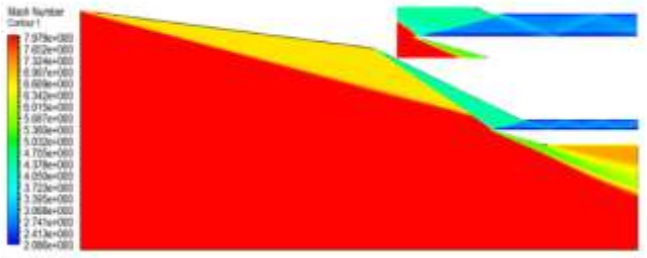

`Fig. 14Mach number contour for case 2 (Mach 8)

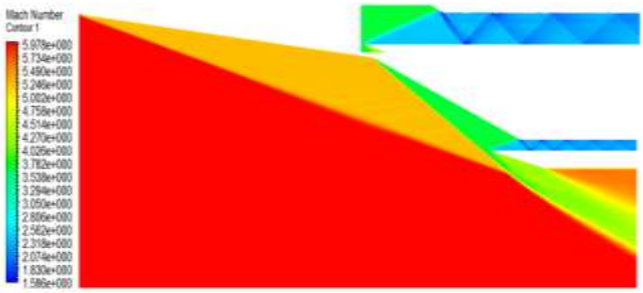

Fig. 15Mach number contour for case 3 (Mach 6)

The numerical calculation of pressure profiles at the isolator exit for the cases of varying Mach number is illustrated in Fig. 16. As can be seen in Figs. 14-15, the pressure variations of case 2 (Mach 8) and case 3 (Mach 6) are almost fluctuated due to several reflected shock inside the isolator and this can affect the combustion process. As predicted, the desired case 1 (Mach 7) and the cases for the changes of flight altitude (case 4 and case 5) occur constant pressure profiles because these cases satisfy the SOL condition.

TABLE II summarizes the validation of calculated results from CFD and the reference results from [12] with percentage

error for the performance parameters at the midpoint of isolator exit from cases 1 to 5. The last two cases (case 4 and case 5) in this table refer to changes in flight altitude. As seen in this table, the performance parameters of the last two cases are almost the same as the case 1 although the effects on the airflow properties are significantly different. The highest kinetic energy efficiency is occurred the cases with SOL condition.

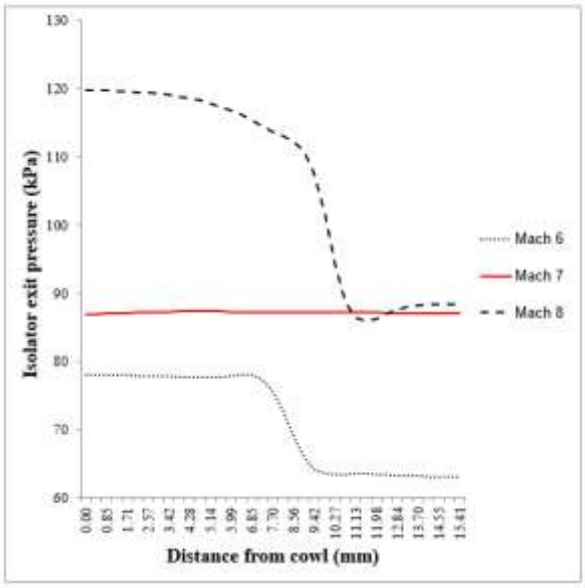

Fig. 16 Pressure profiles at the isolator exit for varying Mach number

TABLE II
VALIDATION OF REFERENCE AND CFD RESULTS FOR PERFORMANCE PARAMETERS AT THE MIDPOINT OF ISOLATOR EXIT

Case	Total pressure recovery			Kinetic energy efficiency		
	Ref.	CFD	% error	Ref.	CFD	% error
1	0.358	0.356	0.558	0.965	0.965	0
2	0.221	0.243	9.053	0.956	0.961	0.520
3	0.404	0.418	3.349	0.959	0.961	0.208
4	0.358	0.356	0.558	0.965	0.965	0
5	0.358	0.356	0.558	0.965	0.965	0

V. CODE DEVELOPMENT FOR SCRAMJET INLET

A. SOL Design Geometry Consideration

As mentioned above, the SOL condition can occur the greater performance parameters for inviscid flow and calorically perfect gas models. The SOL design geometry can be constructed with scramjet inlet design (SID) program which is based on the oblique shock relations. Moreover, it can evaluate the performance parameters and flow properties directly. This program gives initial solution with less computing power, simplest and fastest way for design consideration. The needed design input is less and efficient. The isolator's length, cowl's length, angle and thickness are not considered in SID program. The schematic diagram of general inlet geometry is shown in Fig. 17.

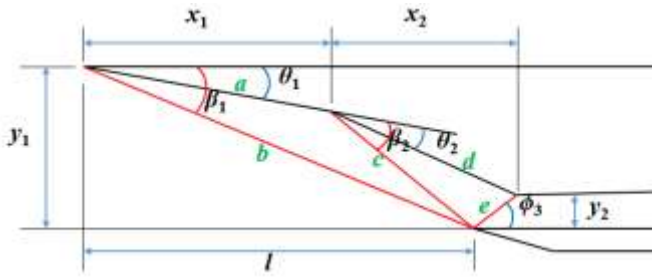

Fig. 17States numbering and nomenclature of scramjet inlet design

B. Design Constraints and Inputs

The SID code utilizes the design constraints which satisfies SOL condition, shock waves are weak oblique shock with attached flow, mixed compression inlet with two ramps and three shock system, the cowl line is horizontal and inlet Mach number is greater than or equal three. The SID program requires the inputs which are design altitude, design Mach number (M_1), turning angle (θ_1) and horizontal distance of first ramp (x_1), the ratio of horizontal length of first ramp and overall height of scramjet inlet (effective geometric ratio = x_1/y_1).

C. Design Methodology

The SID code is developed by the following steps:

INPUTS: $\gamma, \delta, c_p, R, M_1, \theta_1, x_1, x_1/y_1, P_1, T_1$

EQUATIONS: *SOL Design Geometry*

$$l = y_1 \cot\beta_1$$

$$a = \frac{x_1}{\cos\theta_1}$$

$$b = \frac{y_1}{\sin\beta_1}$$

$$c^2 = a^2 + b^2 - 2ab\cos(\beta_1-\theta_1)$$

$$\beta_2 = (\beta_1 - \theta_1) + \sin^{-1}\left[\frac{a\sin(\beta_1 - \theta_1)}{c}\right]$$

$$\tan\theta_2 = 2\cot\beta_2\frac{M_2^2\sin^2\beta_2 - 1}{M_2^2(\gamma + \cos 2\beta_2) + 1}$$

$$\theta_3 = \theta_1 + \theta_2$$

$$\phi_3 = \beta_3 - \theta_3$$

$$d = c\frac{\sin(180 - \beta_2 - \theta_1)}{\sin(\theta_3 - \phi_3)}$$

$$e^2 = c^2 + d^2 - 2cd\cos(\beta_2 - \theta_2)$$

$$x_2 = d\cos\theta_3$$

$$y_2 = e\sin\phi_3$$

Performance Parameters

$$\frac{P_{04}}{P_{01}} = \pi_c = \frac{P_{04}}{P_{03}}\frac{P_{03}}{P_{02}}\frac{P_{02}}{P_{01}}$$

$$\eta_{KE\_ad} = 1 - \frac{2}{(\gamma\text{-}1)M_1^2}\left[\left(\frac{1}{\pi_c}\right)^{\frac{\gamma-1}{\gamma}} - 1\right]$$

$$\frac{P_4}{P_1} = \frac{P_4}{P_3}\frac{P_3}{P_2}\frac{P_2}{P_1}$$

$$\frac{T_4}{T_1} = \frac{T_4}{T_3}\frac{T_3}{T_2}\frac{T_2}{T_1}$$

$$M_4 = \frac{1}{\sin(\beta_3-\theta_3)}\left[\frac{1+\frac{\gamma-1}{2}M_3^2\sin^2\beta_3}{\gamma M_3^2\sin^2\beta_3-\frac{\gamma-1}{2}}\right]^{1/2}$$

OUTPUTS: *SOL design geometry, Performance parameters*

D. Consideration on lowest Mach number 3

The current technical challenge in scramjet inlet design is to achieve SOL condition at Mach 3. Therefore, the SOL geometry for Mach number 3 and inviscid flow were considered for current design. The scramjet inlet design for Mach 3 is calculated with SID program using γ=1.4, δ=1, c_p=1005J/kg K, R=287J/kg K, M_1=3, θ_1=5, x_1=100mm, x_1/y_1=1.2, H=20km (P_1=5.5293kPa, T_1=216.66K).

The dimensional data of SOL geometry calculated by SID program is shown in the following Fig. 18 and performance parameter results are validated by CFD results as shown in TABLEIII.`

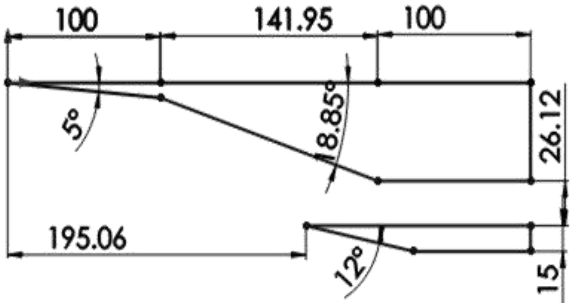

Fig. 18Schematic diagram of SOL geometry calculated by SID program

The lowest Mach number SOL geometry was designed by SID program. The accuracy of SID program is validated by CFD results. As can be seen in TABLEIII, the validation of these two results is confirmed with very small percentage error. Although the scramjet inlet can be run with supersonic Mach number 3, the static temperature appeared to be a problem because the temperature cannot reach the minimum temperature of 1000K. This is due to the free stream Mach number is supersonic and the flow is inviscid but the problem may be minor for combustion process. Many effects of heating can occur in real flow such as boundary layer heating and friction.

The SID program can calculate SOL geometry and performance parameters simultaneously while CFD cannot construct the SOL geometry although it needs more computing power. The Mach contour in Fig. 19 shows the result which satisfies SOL condition at Mach 3. It also shows the results predicted by SID and CFD. The two results are almost equal with maximum percentage error of 0.16.

TABLE III
VALIDATION OF SID PROGRAM AND CFD RESULTS FOR MACH 3 AT MIDPOINT OF ISOLATOR EXIT

	SID	**CFD**	**% error**
Pressure recovery (π_c)	0.8343	0.8356	0.156
Kinetic energy efficiency	0.9705	0.9707	0.02
Geometric contraction ratio	3.1902	3.1902	-
Pressure ratio (P_4/P_1)	9.7972	9.7887	0.087
Temperature ratio (T_4/T_1)	2.0207	2.0174	0.163
P_4 (kPa)	54.171	54.125	0.083
T_4 (K)	437.78	437.1	0.156
M_4	1.3886	1.39	0.1

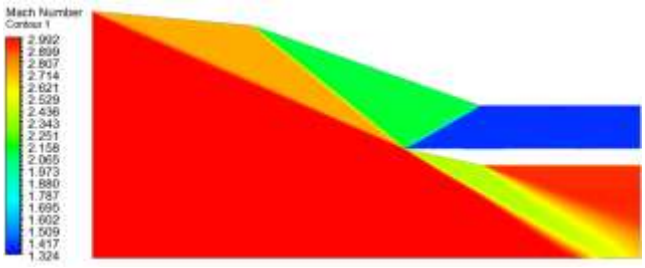

Fig. 19Mach number contour for Mach 3

VI. CONCLUSION

Firstly, the suitable mixed compression inlet geometry was chosen from various geometries. For dimensional data, the reference intake design, which is the first Brazilian hypersonic vehicle prototype, the 14-X airplane, with the cases 1 to 5 (TABLEI)was selected. For numerical investigation, the design constraints, computational domains, grid independent checking and other factors were defined. And then, the results of CFD were validated with the results of oblique shock relations and the results of [12] and found good agreement. From this numerical investigation, the performance and flow properties were found to be the best when the inlet satisfies SOL condition.

Therefore, SID program was developed to construct SOL geometry and calculate flow properties and performance parameters. Moreover, the lowest Mach number starting inlet, one of the technical challenge for a hybrid turbojet-scramjet, was designed and tested by CFD. The accuracy of SID program results were validated by CFD results and it showed very small error percentage.

Therefore, in-house scramjet inlet design program is found to be useful in designing a new scramjet inlet and can be used to make an initial analysis of designed inlet before using more expensive tools like CFD.

ACKNOWLEDGMENT

The author would like to acknowledge Dr. Aung Myo Thu for many insightful conversations and comments. And also thank U Than Swe for helping anything we need. This work was supported by Fluid Energy and Environmental Engineering lab, FEELab.

REFERENCES

[1] Michael K. Smart, "Scramjet inlets," Centre for Hypersonics, The University of Queensland Brisbane 4071, Australia, September 2010.

[2] Fry, Ronald S. "A Century of Ramjet Propulsion Technology Evolution,"Journal of Propulsion and Power, Volume 20, No. 1, January-February 2004: 27-58.

[3] "HyShot Program Secures Place in Flight History." The University of Queensland in Australia. 16 Aug. 2002.

[4] Thompson, Elvia, Keith Henry, and Leslie Williams. "Faster Than a Speeding Bullet: Guinness Recognizes NASA Scramjet." NASA. 20 June 2005.

[5] Anderson, John D., Jr., "Fundamentals of Aerodynamics," 5th Edition, the McGraw-Hill Companies, Inc, New York, 2011.

[6] David M. Van Wie, Stephen M. D'Alessio, and Michael E. WhiteJ, "Hypersonic Airbreathing Propulsion,"Johns Hopkins APL Technical Digest, Volume 26, Number 4, 2005.

[7] Kristen Nicole Roberts, "Analysis and Design of a Hypersonic Scramjet Engine with a Starting MachNumber of 4.00," August 2008.

[8] Jason Paur, "Hypersonic Successor to Legendary SR-71 Blackbird Spy Plane Unveiled*,"*Wired, 1 November 2013.

[9] Corin Segal, "The Scramjet Engine: Processes and Characteristics," Cambridge University Press, New York, 2009.

[10] D. M. Van Wie, M. E. White, and G. P. Corpening, "NASP (National Aero Space Plane) Inlet Design And Testing Issues," Johns Hopkins APL Technical Digest, Volume 11, Numbers 3 and 4, 1990.

[11] Luu Hong Quan, Nguyen Phu Hung, Le Doan Quang, Vu Ngoc Long,"Analysis and Design of a Scramjet Engine Inlet Operating from Mach 5 to Mach 10,"*International Journal of Mechanical Engineering and Applications.* Vol. 4, No. 1, 2016, pp. 11-23.

[12] Augusto F. Moura, Maurício A. P. Rosa, "A Numerical Investigation of Scramjet Engine Air Intakes for the 14-X Hypersonic Vehicle".

[13] Anderson, John D., Jr., "Modern Compressible Flow: With Historical Perspective," 3rd Edition, McGraw-Hill Book Company, New York, 2003.

[14] Azam CheIdris, Mohd Rashdan Saad, Hossein Zare-Behtash, Konstantinos Kontis, "Luminescent Measurement Systems for the Investigation of a Scramjet Inlet-Isolator," 9 April 2014.

AUTHORS

Phyo Wai Thaw
B.E (Aerospace)
Department of Propulsion and Flight Vehicles
Myanmar Aerospace Engineering University

Zin Win Thu
B.E (Aerospace)
Department of Propulsion and Flight Vehicles
Myanmar Aerospace Engineering University